Research Square

Preprints are preliminary reports that have not undergone peer review.
They should not be considered conclusive, used to inform clinical practice,
or referenced by the media as validated information.

Mechanistic Study of Deoxyshikonin-Mediated Protection Against High-Glucose-Induced Injury in HUVECs

Chao Bai
First Affiliated Hospital of Xinjiang Medical University
Wenwen Yang
First Affiliated Hospital of Xinjiang Medical University
Xiaoyun Ni
First Affiliated Hospital of Xinjiang Medical University
Pengfei Xu
First Affiliated Hospital of Xinjiang Medical University
Tuerdebieke Jiakesileke
First Affiliated Hospital of Xinjiang Medical University
Shuyao Li
First Affiliated Hospital of Xinjiang Medical University
Tao Liu
liutao@xjmu.edu.cn

Xinjiang Medical University

Article

Keywords: deoxyshikonin, high-glucose microenvironment, human umbilical vein endothelial cells, endothelial dysfunction, angiogenesis

Posted Date: August 12th, 2026

DOI: https://doi.org/10.21203/rs.3.rs-10221671/v1

License: This work is licensed under a Creative Commons Attribution 4.0 International License.
Read Full License

Additional Declarations: No competing interests reported.

Mechanistic Study of Deoxyshikonin-Mediated Protection Against High-Glucose-Induced Injury in HUVECs

Chao Bai[1], Wenwen Yang[2], Xiaoyun Ni[1],Pengfei Xu[1], Tuerdebieke Jiakesileke[1], Shuyao Li[1], Tao Liu[3]*

[1] Department of Vascular and Thyroid Surgery, The First Affiliated Hospital of Xinjiang Medical University, Urumqi 830054, Xinjiang, China;

[2] Department of Clinical Nutrition, The First Affiliated Hospital of Xinjiang Medical University, Urumqi 830054, Xinjiang, China;

[3] School of Public Health, Xinjiang Medical University, Urumqi 830000, Xinjiang, China;

* Corresponding author: Tao Liu, MD, School of Public Health, Xinjiang Medical University, No. 567 Shangde North Road, Shuimogou District, Urumqi 830017, Xinjiang, China. Tel: +86-18997956799. E-mail: liutao@xjmu.edu.cn

Running title: Deoxyshikonin Protects HUVECs Under High Glucose

Funding Statement:

This study was supported by the Xinjiang Uygur Autonomous Region "Tianshan Talent" Top Young Talent Program—Youth Science and Technology Innovation Talent Project (Grant No. 2023TSYCCX0053), the Tianshan Innovation Team Program of the Science and Technology Department of Xinjiang Uygur Autonomous Region (Grant No. 2025D14021), and the Xinjiang Uygur Autonomous Region Natural Science Foundation—Outstanding Youth Science Fund Project (Grant No. 2025D01041).

Conflict of Interest Statement:

The authors declare no conflict of interest.

Data Availability Statement:

All raw data from our manuscript have been successfully uploaded to the Gene Expression Omnibus (GEO) database. The GEO accession number assigned is GSE338148. We have generated a secure review token for the private GSE record GSE338148 to facilitate editorial evaluation. The valid review token is **khudyimgpzedpmx**. Access it through this link

{https://www.ncbi.nlm.nih.gov/geo/query/acc.cgi?acc=GSE338148}, which allows full access to the dataset during the peer review period. The relevant sequencing data of this study has not been publicly released yet.

Abstract

Objective: This study aimed to elucidate the mechanism by which deoxyshikonin (DS) ameliorates high-glucose-induced injury in human umbilical vein endothelial cells (HUVECs).

Methods: HUVECs were treated with different concentrations of DS, and cytotoxicity was assessed to determine a safe working concentration. A stable high-glucose injury model was established by exposing HUVECs to different glucose concentrations. Cells were then divided into a normal control group (5.5 mM glucose), a high-glucose (HG) model group (100 mM glucose), and a DS intervention group (100 mM glucose + 3 μM DS), followed by functional assessment using a Matrigel tube formation assay. RNA sequencing was performed in the control, HG, and HG+DS groups to identify differentially expressed genes (DEGs), and Gene Ontology (GO) and Kyoto Encyclopedia of Genes and Genomes (KEGG) enrichment analyses were conducted. Candidate downstream effectors were selected based on sequencing data and literature evidence and validated by reverse-transcription quantitative PCR (RT-qPCR).

Results: DS at 3 μM showed no cytotoxicity in HUVECs and was selected for subsequent experiments. Exposure to 100 mM glucose significantly inhibited HUVEC viability and increased apoptosis ($P < 0.05$), whereas mannitol controls showed no comparable effect, excluding osmotic interference. High glucose markedly impaired tube formation compared with the control group ($P < 0.05$), while DS treatment significantly restored angiogenic capacity ($P < 0.05$). Transcriptomic analysis identified 173 DEGs between the HG and control groups, including 91 upregulated and 82 downregulated genes. A total of 2,015 DEGs were identified between the HG+DS and HG groups, including 975 upregulated and 1,040 downregulated genes. GO and KEGG analyses indicated that DS-regulated genes were enriched in extracellular matrix organization, cell adhesion, inflammatory response, angiogenesis-related biological processes, ECM-receptor interaction, AGE-RAGE signaling, focal adhesion, cell cycle, proteasome, and arachidonic acid metabolism. RT-qPCR validation showed that IFITM1, THY1, CCBE1, CCL2, and ENTPD1 were upregulated after high-glucose exposure and were downregulated after DS intervention.

Conclusion: DS at 3 μM ameliorates high-glucose-induced endothelial dysfunction in HUVECs. IFITM1, THY1, CCBE1, CCL2, and ENTPD1 may act as key downstream effectors through which DS exerts endothelial-protective effects.

Keywords: deoxyshikonin; high-glucose microenvironment; human umbilical vein endothelial cells; endothelial dysfunction; angiogenesis

1. Introduction

Diabetes mellitus is a chronic metabolic disease with a continuously increasing incidence and prevalence worldwide, and its vascular complications are a major cause of disability and mortality [1,2]. Long-term hyperglycemia can lead to multiple complications. In the early stage, diabetic neuropathy, typically manifested as reduced sensation in the lower extremities, may result in a "high-risk diabetic foot" condition [3]. As the disease progresses, vascular endothelial dysfunction in the lower limbs and diabetes-related cardiovascular disease may occur, eventually leading to foot ulceration and limb necrosis [4,5]. In a high-glucose environment, endothelial cells exhibit reduced proliferative capacity, increased apoptosis, impaired migration, and defective angiogenesis; collectively, these phenotypic changes contribute to the onset and progression of diabetic vascular disease [6,7].

Hyperglycemia injures endothelial cells through multiple mechanisms, including oxidative stress, inflammatory responses, protein kinase C activation, and mitochondrial dysfunction [8,9]. Dysregulation of vascular endothelial growth factor (VEGF) signaling is closely associated with impaired angiogenesis in diabetes, resulting in defective tissue repair [10].

Deoxyshikonin (DS) is a natural naphthoquinone compound mainly isolated from the dried roots of Lithospermum erythrorhizon, a traditional Chinese medicinal herb known as Zicao [11]. DS has been reported to exert multiple biological effects, including anti-inflammatory and antioxidant activities, promotion of wound healing, superoxide anion scavenging, and attenuation of oxidative-stress-induced cellular injury [12,13]. In a mouse model of diabetic wounds, DS promoted angiogenesis by upregulating VEGFR2 expression and enhancing Akt/p38 phosphorylation [10]. DS may also regulate HIF-1α expression and nuclear translocation, thereby promoting tube formation in lymphatic endothelial cells [14,15]. These findings provide a theoretical basis for the potential clinical application of DS in diabetic vascular complications. In recent years, Bai et al. found through high-throughput sequencing that certain molecules were markedly upregulated in diabetic foot ulcer

tissues; these molecules could be suppressed by DS, thereby enhancing tube formation in diabetic foot ulcer tissue and contributing to wound repair [16].

However, the mechanism by which DS promotes angiogenesis under high-glucose conditions remains unclear. In the present study, we established a high-glucose-induced HUVEC injury model, evaluated the protective effects of DS, and used high-throughput sequencing to identify DS-regulated key pathways and downstream effector molecules. This study further clarifies the molecular mechanisms involved in diabetic foot ulcers and provides a theoretical basis for DS-mediated repair of injured tissue.

2. Materials and Methods

2.1. Drug treatment and safety evaluation

Deoxyshikonin (DS; purity ≥98%) was purchased from Sigma-Aldrich and dissolved in dimethyl sulfoxide (DMSO). HUVECs were treated with DS at final concentrations of 0, 3, 6, and 10 μM for 24 or 48 h. Cell viability was assessed using the Cell Counting Kit-8 (CCK-8) assay to determine a safe concentration range for subsequent experiments.

2.2. Cell culture and establishment of the high-glucose model

Human umbilical vein endothelial cells (HUVECs) were purchased from Shanghai Zhong Qiao Xin Zhou Biotechnology Co., Ltd. Cells were cultured in ECSM medium supplemented with 10% fetal bovine serum (Gibco), 100 U/mL penicillin, and 100 μg/mL streptomycin (HyClone) at 37 °C in a humidified incubator containing 5% CO_2. To establish a high-glucose injury model, cells were exposed to 100 mM glucose for 48 h. Cells cultured with 5.5 mM glucose served as the normal control, and mannitol at corresponding concentrations was used as an osmotic control.

2.3. Cell functional assays

CCK-8 assay: HUVECs were seeded into 96-well plates at a density of 10,000 cells per well. After the indicated treatments, 10 μL of CCK-8 solution was added to each well, and cells were incubated at 37 °C for 3 h. Absorbance was measured at 450 nm.

Flow-cytometric analysis of apoptosis: Apoptosis was assessed using an Annexin V-APC/7-AAD apoptosis detection kit. After treatment, cells were stained according to the manufacturer's instructions, and the apoptotic rate was analyzed using a flow cytometer (FACSCanto, BD Biosciences).

Wound-healing assay: Cells were cultured to approximately 90% confluence, and a sterile pipette tip was used to create a linear scratch. After washing with phosphate-buffered saline (PBS), wound closure was observed at 0 and 21 h. Migration rates were calculated using ImageJ software.

Tube formation assay: HUVECs were seeded into 24-well plates pre-coated with Matrigel and incubated at 37 °C for 3 h. The numbers of branches and junctions were then quantified.

2.4. Transcriptome sequencing and data analysis

Total RNA was extracted from HUVECs in each group. RNA-seq libraries were constructed using the VAHTS Universal V8 RNA-seq Library Prep Kit and sequenced on the Illumina NovaSeq 6000 platform. Differentially expressed genes (DEGs) were identified using the criteria $|\log_2 \text{fold change}| > 1$ and $P < 0.05$. GO and KEGG enrichment analyses were performed using the KOBAS 2.0 server[28,29].

2.5. Reverse-transcription quantitative PCR (RT-qPCR)

Total RNA was extracted from cells in each group and reverse-transcribed into cDNA. qPCR was performed using SYBR Green Master Mix on a QuantStudio 5 Real-Time PCR System. GAPDH was used as the internal reference gene. Candidate genes included IFITM1, THY1, CCBE1, CCL2, and ENTPD1. Relative expression levels were calculated using the $2^{-\Delta\Delta Ct}$ method [18].

2.6. Statistical analysis

All experiments were independently repeated three times. Data are presented as the mean ± standard deviation (SD). Comparisons between two groups were performed using a two-tailed Student's t-test, and comparisons among multiple groups were performed using one-way analysis of variance. $P < 0.05$ was considered statistically significant.

3. Results

3.1. Cytotoxicity and safety evaluation of DS in HUVECs

To determine a safe working concentration of DS, HUVECs were treated with 0, 3, 6, or 10 μM DS. Morphological observation and CCK-8 analysis showed that DS did not cause obvious cytotoxicity at these concentrations. Among the tested concentrations, 3 μM DS maintained favorable cell viability and was therefore selected for subsequent intervention experiments (Figure 1).

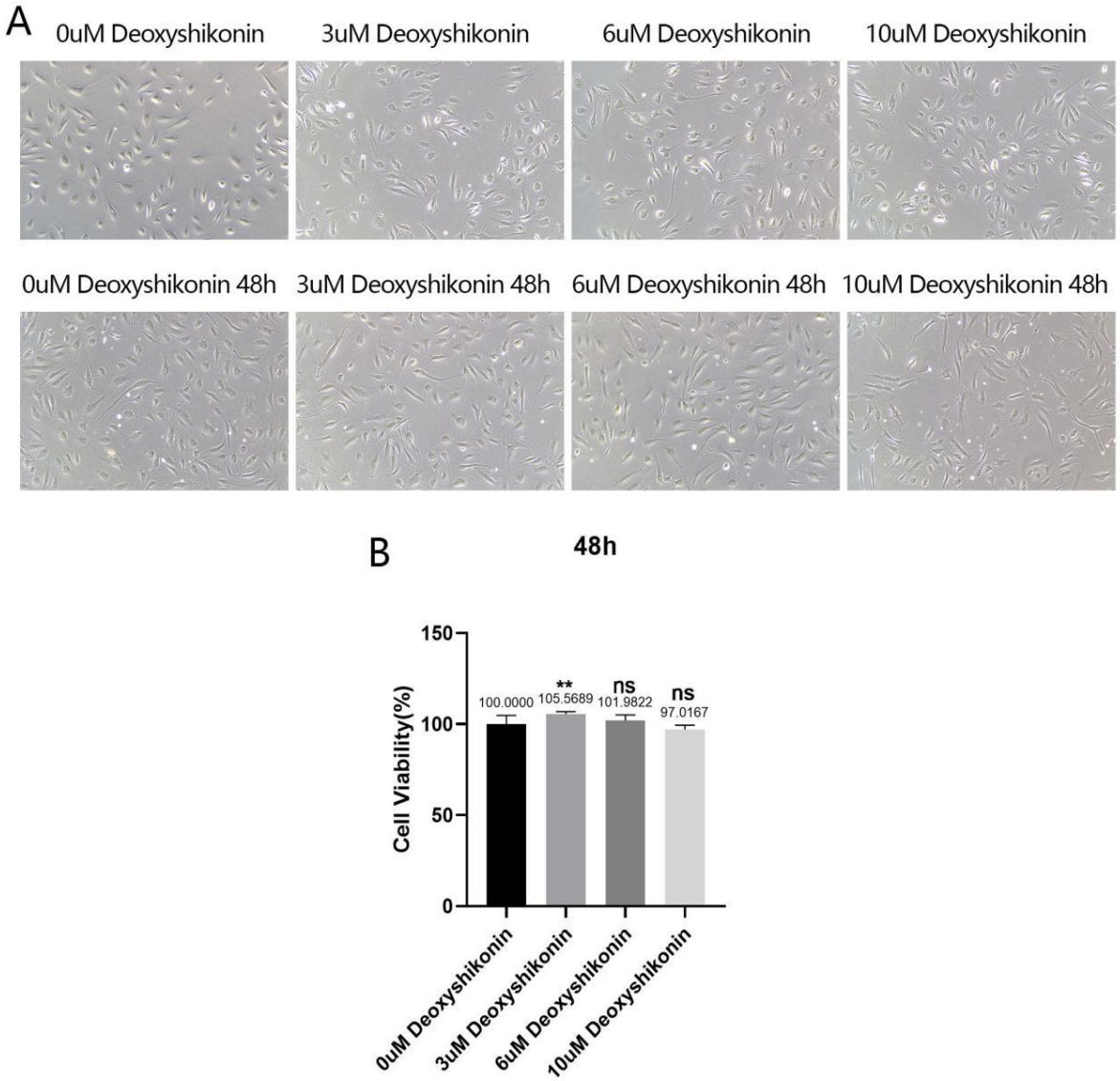


Figure 1. Safety evaluation of DS in HUVECs. (A) Representative microscopic images of HUVECs treated with 0, 3, 6, or 10 μM DS, including observations after 48 h. (B) CCK-8 assay showing cell viability after DS treatment for 48 h. Data are presented as the mean ± SD (n = 3). **P < 0.01; ns, not significant.

3.2. Establishment of a high-glucose-induced HUVEC injury model

To establish a stable and reliable high-glucose injury model, HUVECs were exposed to different concentrations of glucose for 48 h, with corresponding mannitol controls used to exclude osmotic effects. High-glucose treatment increased the apoptotic rate of HUVECs in a concentration-dependent manner, whereas the mannitol control groups did not show comparable pro-apoptotic effects. Exposure to 100 mM glucose produced a marked and reproducible apoptotic response while preserving sufficient cells for subsequent functional assays; therefore, 100 mM glucose for 48 h was selected as the high-glucose model condition (Figure 2).

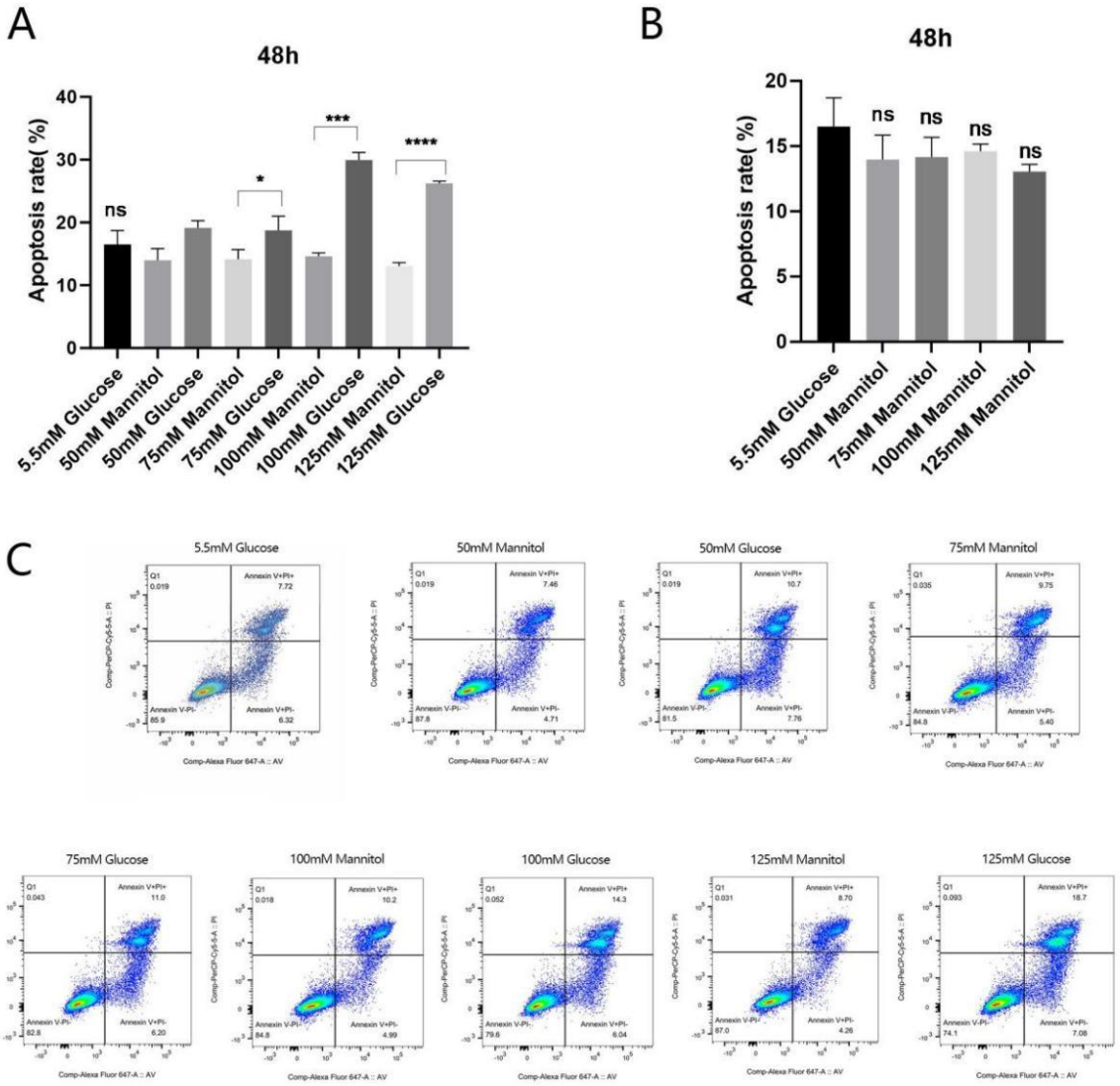


Figure 2. Establishment of the high-glucose-induced HUVEC injury model. HUVECs were exposed to different concentrations of glucose or corresponding mannitol controls for 48 h. (A) Quantitative analysis of apoptosis after glucose or mannitol treatment. (B) Apoptosis rates in mannitol control groups. (C) Representative flow-cytometry plots from Annexin V-APC/7-AAD staining. Data are presented as the mean ± SD (n = 3). *P < 0.05, ***P < 0.001, ****P < 0.0001; ns, not significant.

3.3. DS restores tube formation in HUVECs under high-glucose conditions

To evaluate the endothelial-protective effect of DS, HUVECs were divided into three groups: control (5.5 mM glucose), HG (100 mM glucose), and HG+DS (100 mM glucose + 3 μM DS). Matrigel tube formation assays showed that 100 mM glucose markedly suppressed the angiogenic capacity of HUVECs, as reflected by reductions in the numbers of branches and junctions. Compared with the HG group, the HG+DS group exhibited significantly increased branch and junction numbers ($P < 0.05$), indicating that DS reversed high-glucose-induced impairment of angiogenesis (Figure 3).

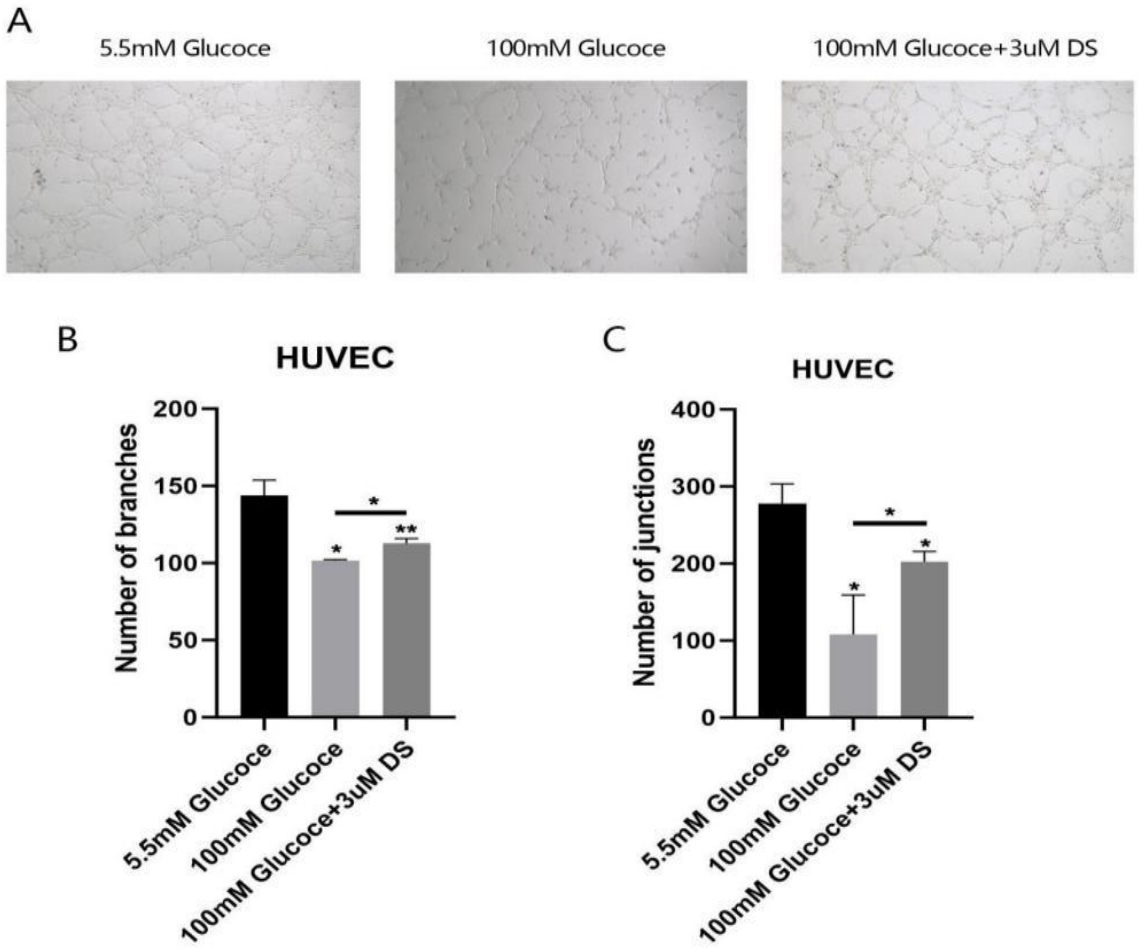


Figure 3. DS reverses high-glucose-induced impairment of angiogenesis in HUVECs. (A) Representative images of tube formation in the control, HG, and HG+DS groups. (B) Quantification of branch numbers. (C) Quantification of junction numbers. Data are presented as the mean ± SD (n = 3). *P < 0.05, **P < 0.01.

3.4. Transcriptomic profiling identifies DS-regulated differentially expressed genes

To systematically investigate the molecular mechanism of DS, RNA sequencing was performed in the control, HG, and HG+DS groups. The overall transcriptomic profiles showed clear grouping among samples. Compared with the control group, the HG group exhibited 173 DEGs, including 91 upregulated and 82 downregulated genes. Compared with the HG group, the HG+DS group exhibited 2,015 DEGs, including 975 upregulated and 1,040 downregulated genes (Figure 4). These results indicate that high-glucose stimulation significantly alters the HUVEC transcriptomic profile and that DS intervention reverses or modulates a substantial subset of these abnormal expression changes.

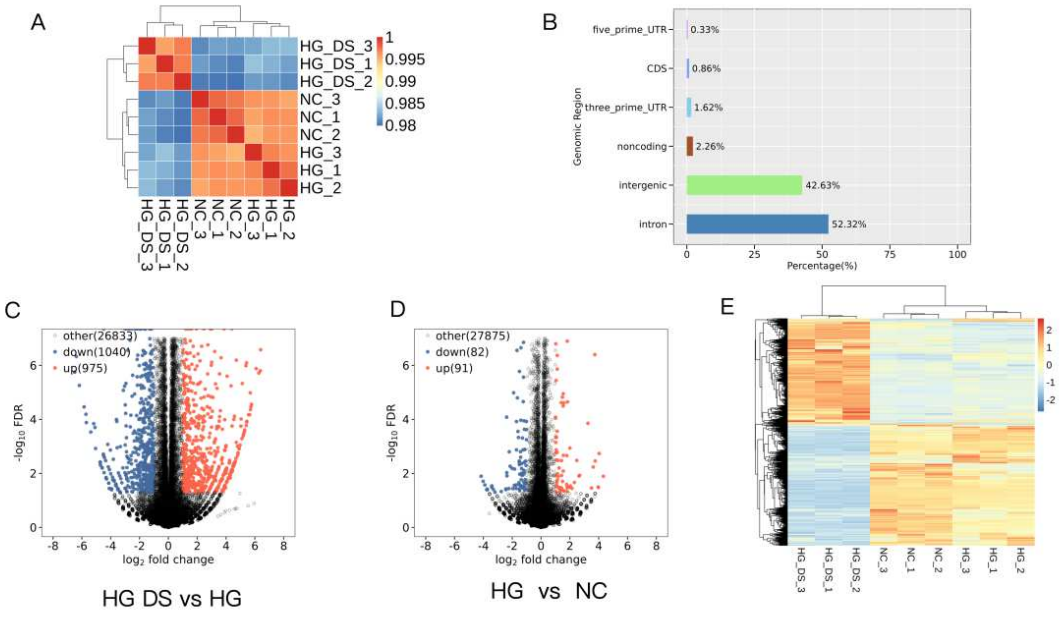


Figure 4. Transcriptomic profiling of HUVECs in the control, HG, and HG+DS groups. (A) Sample correlation heatmap. (B) Genomic distribution of mapped reads. (C) Volcano plot of DEGs in the HG+DS versus HG comparison, showing 975 upregulated and 1,040 downregulated genes. (D) Volcano plot of DEGs in the HG versus normal control (NC) comparison, showing 91 upregulated and 82 downregulated genes. (E) Heatmap showing clustering of differentially expressed genes. The screening threshold was $|\log_2 \text{fold change}| > 1$ and $P < 0.05$.

To further define the biological functions and signaling pathways regulated by DS, DEGs from the HG+DS versus HG comparison were subjected to GO functional annotation and KEGG pathway enrichment analyses. GO analysis showed that DS-downregulated genes were mainly enriched in cellular components and biological processes such as extracellular space, extracellular region, extracellular matrix, plasma membrane, cell adhesion, angiogenesis, extracellular matrix organization, mitotic cell cycle, and collagen fibril organization. DS-upregulated genes were mainly enriched in extracellular exosomes, cytoplasm, extracellular region, plasma membrane, proteasome complex, signal transduction, inflammatory response, chemotaxis, response to lipopolysaccharide, cell adhesion, and cell-matrix adhesion. Molecular-function terms included protein binding, calcium ion binding, extracellular matrix structural constituent, ATP binding, actin binding, collagen binding, and integrin binding (Figure 5A-F).

KEGG pathway enrichment analysis indicated that DS-regulated DEGs were significantly enriched in pathways related to ECM-receptor interaction, malaria, axon guidance, cell cycle, protein digestion and absorption, p53 signaling, focal adhesion, AGE-RAGE signaling in diabetic complications, cell adhesion molecules, FoxO signaling, proteasome, biosynthesis of amino acids, ferroptosis, hematopoietic cell lineage, glutathione metabolism, fructose and mannose metabolism,

phagosome, rheumatoid arthritis, fluid shear stress and atherosclerosis, and arachidonic acid metabolism (Figure 5G,H). These pathways are closely associated with extracellular matrix remodeling, inflammation, oxidative stress, cell death, and angiogenesis, suggesting that DS may exert endothelial-protective effects through coordinated regulation of multiple biological processes.

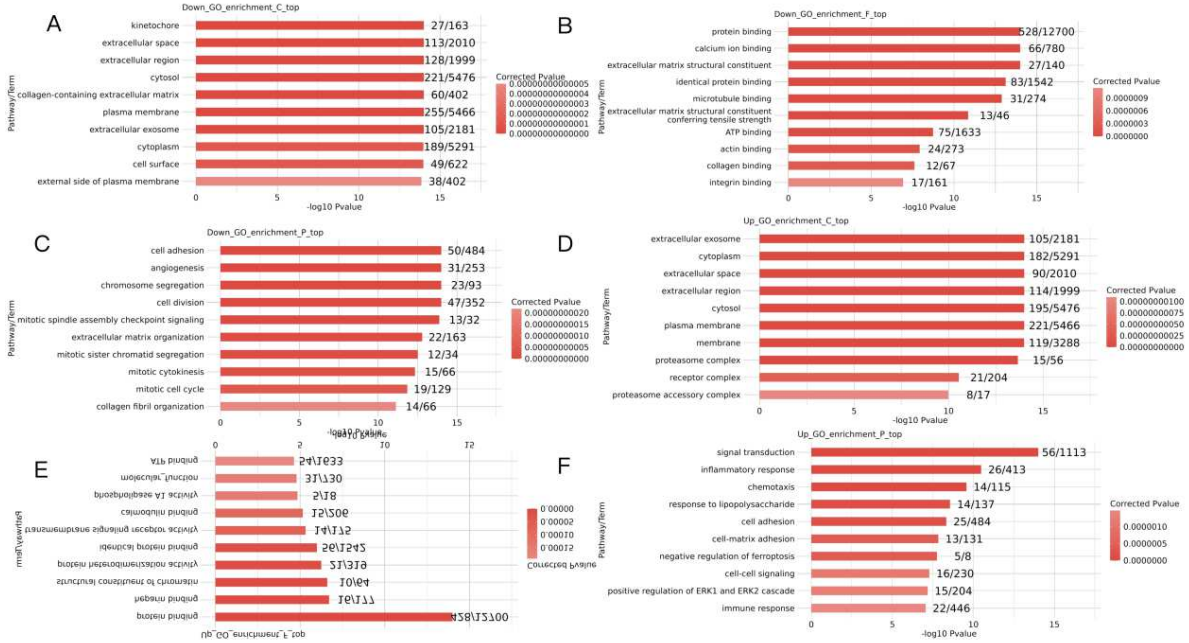


Figure 5. GO enrichment analysis of DS-regulated DEGs. (A-C) Top enriched cellular component, molecular function, and biological process terms among downregulated genes. (D-F) Top enriched cellular component, molecular function, and biological process terms among upregulated genes. The x-axis represents −log10 P value, and the labels indicate the number of enriched genes and total annotated genes for each term.

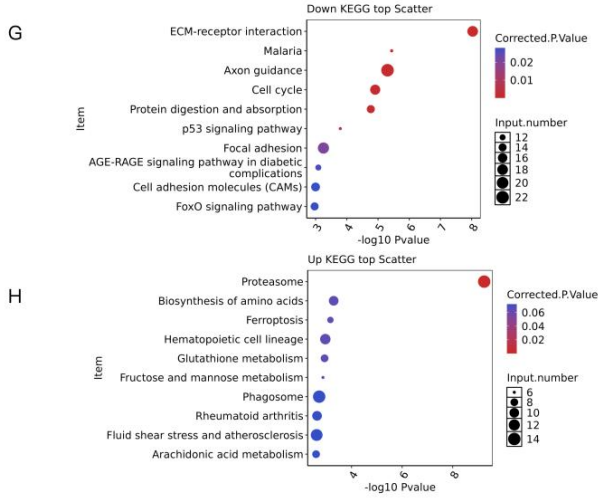


Figure 5 continued. KEGG pathway enrichment analysis of DS-regulated DEGs. (G) Top KEGG pathways enriched among downregulated genes. (H) Top KEGG pathways enriched among upregulated genes. Dot size represents the number of enriched genes, and color indicates the corrected P value.

3.5. Validation of downstream effector genes by RT-qPCR

Based on the high-throughput sequencing data and literature evidence, IFITM1, THY1, CCBE1, CCL2, and ENTPD1 were selected as potential downstream effectors. RT-qPCR was performed to validate their expression patterns in each group. The results showed that IFITM1, THY1, CCBE1, CCL2, and ENTPD1 were significantly upregulated after high-glucose treatment, whereas DS intervention markedly downregulated the expression of these genes (Figure 6). These findings suggest that DS may exert endothelial-protective effects by regulating these key downstream effector molecules.

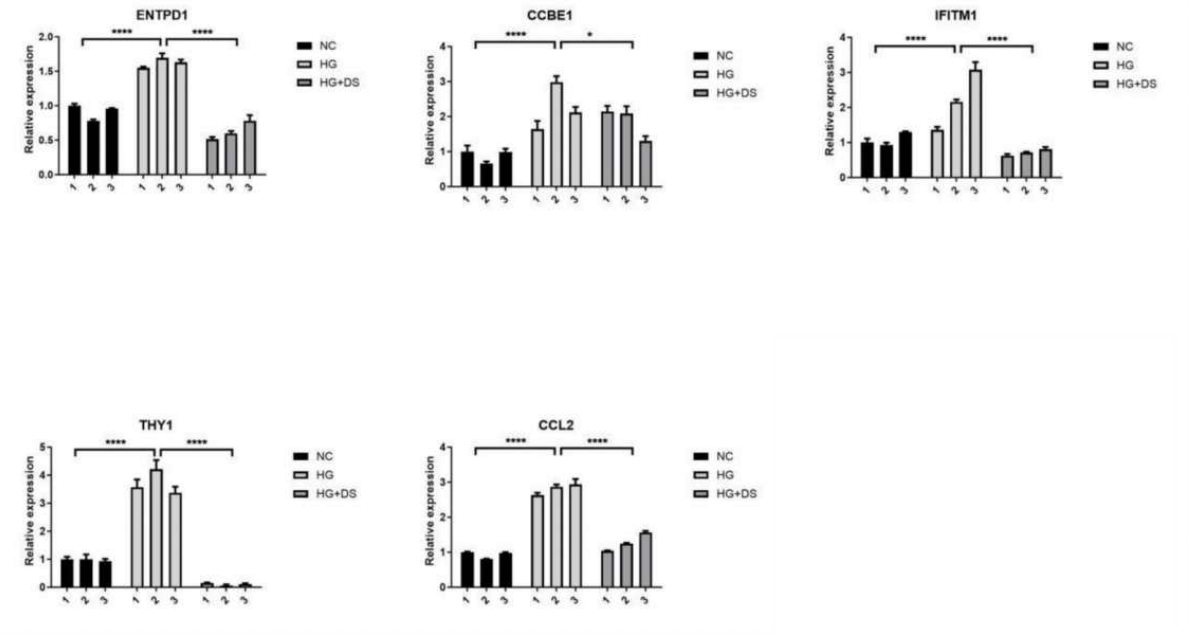


Figure 6. RT-qPCR validation of key gene expression in HUVECs. Cells were divided into the normal control group (NC; 5.5 mM glucose), high-glucose model group (HG; 100 mM glucose), and deoxyshikonin intervention group (HG+DS; 100 mM glucose + 3 μM DS). GAPDH was used as the internal control, and relative mRNA expression levels of IFITM1, THY1, CCBE1, CCL2, and ENTPD1 were calculated using the $2^{-\Delta\Delta Ct}$ method. Each experiment was independently repeated three times. Data are presented as the mean ± SD. *P < 0.05, ****P < 0.0001.

4. Discussion

Diabetic foot ulcers are associated with substantial clinical harm, including high rates of recurrence, amputation, and mortality. Many patients have already lost the opportunity for endovascular or bypass revascularization when they present for treatment. Therefore, direct intervention at the wound surface represents a clinically relevant therapeutic strategy.

Endothelial dysfunction under high-glucose conditions is a central pathological process in diabetic vascular complications. In the present study, we systematically evaluated the protective

effect of DS against high-glucose-induced HUVEC injury and preliminarily elucidated its molecular mechanism through high-throughput sequencing. First, we confirmed that 3 μM DS had minimal cytotoxicity toward HUVECs. Second, treatment with 100 mM glucose for 48 h successfully established a stable endothelial injury model, consistent with previously reported high-glucose-induced endothelial injury conditions [19]. Third, tube formation assays in the control, HG, and HG+DS groups demonstrated that 3 μM DS significantly restored the angiogenic capacity of HUVECs under high-glucose conditions. Fourth, transcriptomic sequencing was performed in the three groups, and DEGs were identified through intergroup comparisons, followed by GO and KEGG enrichment analyses. Finally, on the basis of sequencing results and literature review, IFITM1, THY1, CCBE1, CCL2, and ENTPD1 were selected as candidate downstream effector genes and experimentally validated.

IFITM1 (interferon-induced transmembrane protein 1) plays an important role in angiogenesis, and previous studies have suggested that IFITM1 is critical for the formation of functional blood vessels. Wang et al. analyzed public diabetic foot ulcer datasets and validated their findings experimentally, showing that IFITM1 was highly expressed in diabetic foot ulcer tissues and could be used to support a diagnostic model for diabetic foot ulcers. THY1 (CD90), a glycosylphosphatidylinositol-anchored protein, is markedly upregulated in endothelial cells during inflammatory-cytokine-induced angiogenesis and has been implicated in wound repair and vascular remodeling [21]. CCBE1 has been identified as a key regulator of lymphangiogenesis [22] and promotes lymphatic endothelial sprouting and migration through the VEGFR3 pathway. Recent evidence indicates that CCBE1 is also expressed in vascular endothelium and may participate in angiogenesis. Although the specific significance of CCBE1 upregulation in high-glucose conditions remains incompletely understood, the reversal effect of DS observed in this study suggests that DS may improve endothelial function partly by regulating CCBE1 expression.

CCL2 (MCP-1) is a key pro-inflammatory chemokine that is upregulated under high-glucose conditions [23]. ENTPD1 (CD39) encodes ectonucleoside triphosphate diphosphohydrolase 1 and plays an important role in inflammation regulation [26]. ENTPD1 hydrolyzes pro-inflammatory extracellular ATP and ADP to AMP, which can subsequently be converted to adenosine by CD73, thereby mediating anti-inflammatory and vasculoprotective effects. In the present study, high-glucose stimulation upregulated ENTPD1 expression, and DS reduced ENTPD1 expression toward the control level. This pattern may reflect a compensatory response to high-glucose-induced inflammatory stress and its attenuation after DS treatment. Together, the DS-mediated reversal of

IFITM1, THY1, CCBE1, CCL2, and ENTPD1 expression suggests that DS may protect the endothelium by regulating inflammation, angiogenic remodeling, and extracellular matrix-related processes.

In recent years, multiple studies have revealed regulatory networks involving key molecules in diabetic vascular complications from different perspectives, complementing the findings of the present study. The current results are also consistent with the reported biological activities of DS. For example, DS has been shown to promote wound healing in diabetic mice through the VEGFR2/Akt/p38 pathway [10], and shikonin derivatives have well-documented anti-inflammatory and antioxidant properties [12,13].

This study has several limitations. First, the direct molecular targets of DS were not validated using gene knockdown or overexpression experiments. Second, the study was mainly based on a single cell type, HUVECs, whereas the complex microenvironment of diabetic foot ulcers involves interactions among multiple cell types [27]. Third, in vivo animal experiments were not performed. Future studies should combine target validation, gain- and loss-of-function experiments, and animal models to further confirm the endothelial-protective mechanism of DS.

In conclusion, the present data indicate that DS may ameliorate high-glucose-induced endothelial dysfunction by regulating downstream effector genes, including IFITM1, THY1, CCBE1, CCL2, and ENTPD1. This study provides multi-omics-based theoretical evidence supporting the therapeutic potential of DS in diabetes-related endothelial injury.

5. References

[1] Ogurtsova K, Guariguata L, Barengo NC, et al. IDF diabetes atlas: Global estimates of undiagnosed diabetes in adults for 2021. Diabetes Res Clin Pract. 2022;183:109118.

[2] Saeedi P, Petersohn I, Salpea P, et al. Global and regional diabetes prevalence estimates for 2019 and projections for 2030 and 2045: Results from the International Diabetes Federation Diabetes Atlas, 9th edition. Diabetes Res Clin Pract. 2019;157:107843.

[3] Bai C, Yang W, Yan J, Qi G, Yang L, Wu Q, Peng J, Luo J, Liu T. Overexpression of hsa-HLA-DRB1 may delay diabetic wound healing and angiogenesis by regulating miRNA_12118 and FLT-1. Sci Rep. 2025;15:18409.

[4] Sardu C, Paolisso P, Sacra C, et al. Effects of metformin therapy on coronary endothelial dysfunction in patients with prediabetes with stable angina and nonobstructive coronary artery stenosis: The CODYCE multicenter prospective study. Diabetes Care. 2019;42(10):1946-1955.

[5] Bandyk DF. The diabetic foot: Pathophysiology, evaluation, and treatment. Semin Vasc Surg. 2018;31(2-4):43-48.

[6] Kaur R, Kaur M, Singh J. Endothelial dysfunction and diabetic complications: Role of oxidative stress. J Diabetes Metab Disord. 2023;22(2):971-983.

[7] Zheng J, Wang R, Wang Y. New concepts drive the development of delivery tools for sustainable treatment of diabetic complications. Biomed Pharmacother. 2024;171:116206.

[8] Muzurović E, Vujošević S, Dragnić S, et al. Cardiovascular complications of diabetes: From microvascular to macrovascular pathways. J Cardiovasc Dev Dis. 2023;10(9):392.

[9] Arya A, Singh R, Kaur R, et al. The role of oxidative stress in diabetes mellitus-induced vascular endothelial dysfunction. J Diabetes Metab Disord. 2023;22(2):971-983.

[10] Ko JA, Kim SY, Kim HJ, et al. Beneficial effects of deoxyshikonin on delayed wound healing in diabetic mice. Int J Mol Sci. 2018;19(11):3660.

[11] Paul-Traversaz M, Umehara K, Watanabe K, Rachidi W, Sève M, Souard F. Kampo herbal ointments for skin wound healing. Front Pharmacol. 2023;14:1116260. doi:10.3389/fphar.2023.1116260.

[12] Andújar I, Recio MC, Giner RM, et al. Shikonin and its derivatives: Biological activities and therapeutic potential. Front Pharmacol. 2022;13:1010844.

[13] Liang S, Ren K, Li B, Li F, Liang Z, Hu J, Xu B, Zhang A. LncRNA SNHG1 alleviates hypoxia-reoxygenation-induced vascular endothelial cell injury as a competing endogenous RNA through the HIF-1α/VEGF signal pathway. Mol Cell Biochem. 2020;465(1-2):1-11.

[14] Wang L, Li Z, Li L, et al. Emerging target discovery strategies drive the decoding of therapeutic power of natural products. Front Pharmacol. 2025;16:1572542.

[15] Zhang Y, Liu X, Wang J, et al. Advances in natural product mechanism research based on target confirmation and single-cell multi-omics. Sci China Life Sci. 2025.

[16] Bai C, Yang W, Qi G, Yang L, Wu Q, Peng J, Wang N, Liu T. Causal association between matrix metalloproteinases and diabetic neuropathy: A two-sample Mendelian randomization study. Front Endocrinol. 2025;15:1429121.

[17] Huang X, Wang Y, Li S, et al. Integrated transcriptomic and proteomic analyses identify the TLR2-CXCR4 axis as a regulator of endothelial cell migration under simulated microgravity. Front Cell Dev Biol. 2025;13:1502341.

[18] Harshitha R, Arunraj DR. Real-time quantitative PCR: A tool for absolute and relative quantification. Biochem Mol Biol Educ. 2021;49(5):800-812.

[19] Pan D, Xu L, Guo M. The role of protein kinase C in diabetic microvascular complications. Front Endocrinol (Lausanne). 2022;13:973058.

[20] Chen X, Xie N, Feng L, Huang Y, Wu Y, Zhu H, Tang J, Zhang Y. Oxidative stress in diabetes mellitus and its complications: From pathophysiology to therapeutic strategies. Chin Med J (Engl). 2025;138(1):15-27.

[21] The GPI-anchored protein Thy-1/CD90 promotes wound healing upon injury to the skin by enhancing skin perfusion. Int J Mol Sci. 2022;23(20):12539.

[22] Lammert E, Hermansson A, Betsholtz C. CCBE1 is required for lymphatic endothelial cell budding and migration. Nature. 2012;491(7424):417-421.

[23] Hu S, Liu M, Bennett S, Wang Z, Pfleger KDG, Xu J. The molecular structure and role of CCL2 (MCP-1) and C-C chemokine receptor CCR2 in skeletal biology and diseases. J Cell Physiol. 2021;236(10):7211-7222.

[24] Liu Z, Guo N, Zhang XJ. Long noncoding TUG1 promotes angiogenesis of HUVECs in preeclampsia via regulating the miR-29a-3p/VEGFA and Ang2/Tie2 pathways. Microvasc Res. 2022;139:104231.

[25] Luo P, Zhang Q, Zhong TY, Chen JY, Zhang JZ, Tian Y, Zheng LH, Yang F, Dai LY, Zou C, Li ZJ, Liu JH, Wang JG. Celastrol mitigates inflammation in sepsis by inhibiting the PKM2-dependent Warburg effect. Mil Med Res. 2022;9(1):22.

[26] Oldach L. A membrane ATPase without transporter activity: Guido Guidotti's laboratory and the search for CD39. J Biol Chem. 2022;298(6):102007. Erratum in: J Biol Chem. 2022;298(8):102244.

[27] Davis FM, Kimball A, Boniakowski A, et al. The role of the immune system in diabetic wound healing. Nat Rev Endocrinol. 2021;17(7):400-414.

[28] Kanehisa, M., Sato, Y., Kawashima, M., Furumichi, M., and Tanabe, M.; KEGG as a reference resource for gene and protein annotation. Nucleic Acids Res. 44, D457-D462 (2016).

[29] Kanehisa, M. and Goto, S.,: KEGG: Kyoto Encyclopedia of Genes and Genomes. Nucleic Acids Res. 28, 27-30 (2000).

Supplementary Files

This is a list of supplementary files associated with this preprint. Click to download.

- KEGGPERMISSION261968.pdf
- KEGGPERMISSION261968.pdf